Turk J Phys
36 (2012) , 385 – 391.

doi:10.3906/fiz-1109-10

Hydrogen implantation effects on the electrical and optical properties of InSe thin films

Atef Fayez QASRAWI[1,2], Khaled Faysal ILAIWI[3] and Antonio POLIMENI[4]
[1] *Group of Physics, Faculty of Engineering, Atılım University, 06836 Ankara-TURKEY*
[2] *Department of Physics, Arab-American University, Jenin, West Bank-PALESTINE*
[3] *Department of Physics, An-najah National University, Jenin, West Bank-PALESTINE*
[4] *Dipartimento di Fisica, Sapienza Universita' di Roma, Piazzale A. Moro 2, 00185 Roma-ITALY*
e-mail: aqasrawi@atilim edu tr

Received: 11.09.2011

Abstract

The effects of hydrogen ion implantation on the structural, electrical and optical properties of amorphous InSe thin films have been investigated. X-ray diffraction analysis revealed no change in the structure of the films. An implantation of 7.3×10^{18} ions/cm^2 decreased the electrical conductivity by three orders of magnitude at 300 K. Similarly, the conductivity activation energy, which was calculated in the temperature range of 300–420 K, decreased from 210 to 78 meV by H-ion implantation. The optical measurements showed that the direct allowed transitions energy band gap of amorphous InSe films has decreased from 1.50 to 0.97 eV by implantation. Furthermore, significant decreases in the dispersion and oscillator energy, static refractive index and static dielectric constants are also observed by hydrogen implantation.

Key Words: Thin films, semiconductors, optical properties, band gap, refractive index

PACS: 71.23.Cq, 78.20.Ci, 78.66.Jg

1. Introduction

Due to their important role in optoelectronic and electronic devices, the fabrication of semiconductor thin films has attracted much attention over last several decades. Films composed of selenium and indium, namely In_xSe_y, thin films have been successfully used in a variety of applications, including solar cell fabrication [1], rectifiers [2, 3], photodiodes [4], gas sensors [5], switching devices [6], detectors [7], and the Li-containing solid state batteries [8].

In our previous investigations we studied the cadmium doping effects on the structural, compositional, electrical, photoconductive and optical properties of polycrystalline InSe thin films. These investigations showed that InSe films are significantly affected by Cd doping [9, 10]. In a more recent work, we have reported the temperature dependence of the optical band gap energy, refractive index, static dielectric constant, and

dispersive oscillator strength and oscillator energy of amorphous undoped InSe thin films [11]. In this work, we report on the dramatic effects exerted by hydrogen incorporation in amorphous InSe thin films, whose properties were previously studied and reported in [11]. In particular, the consequences of H-ions on lattice structure, electrical conduction, direct allowed energy band gap transitions, refractive index, static dielectric constant, dispersion energy and oscillator energy are reported for the first time for InSe. The unavoidable presence of hydrogen in most growth and processing steps of semiconductors makes knowledge of H-related effects particularly important for applications.

2. Experimental details

Powdered α-In_2Se_3 crystal (Aldrich) were used as the thermal evaporation source material. The X-ray diffraction of the source material reveals that the source material (InSe lumps) is polycrystalline α-In_2Se_3 best oriented in the [100] direction. This material also included a minor phase of InSe crystal. The crystal powder was placed in quartz ampoule wound with a molybdenum heating coil, then heated to 800 ± 20 °C under pressure of 10^{-5} Torr. The films were evaporated onto square, ultrasonically cleaned glass substrates (kept at 100 ± 5 °C, to guarantee 1:1 stoichiometric composition), using an appropriate mask for optical and electrical measurements. The thickness of all the films was measured by interferometric method, and were kept around 0.50 ± 0.03 μm. After deposition, for the purpose of post-growth treatment with atomic hydrogen irradiation, the film was inserted into an ion implanter. Hydrogen irradiation was obtained by means of a Kaufman source with the samples held at 200 °C under a vacuum level of about 8×10^{-5} mbar. A low ion energy (100 eV) and low current density (30 μA/cm^2) were employed to reduce sample damage. Different hydrogen doses in the range of 10^{14}–10^{20} ions/cm^2 are applicable. A dose equal 7.3×10^{18} ions/cm^2 was employed for this material. The dose value was determined by measuring the ion beam current through the film area and during specific time duration.

The X-ray diffractograms were recorded using a diffractometer employing Cu-Kα radiation of wavelength 1.54178 Å. The films morphology and composition were studied by a JSM 6400 scanning electron microscope employing an X-ray energy dispersive analyzer. The absorption spectra are recorded at room using a UV-VIS spectrophotometer. The electrical measurements were carried out by using the Hall bar technique in the temperature region of 300–420 K. For this purpose, the current (I) was registered using a MASTECH MS8209 digital multimeter, the voltage V was supplied from PHYWE high resolution voltage source (0–600 V). The conductivity σ of the samples was determined from the relation, $\sigma = ((VA)/(IL))^{-1}$ with A and L being the cross-sectional area and the length of the film.

3. Results and discussion

The structure of InSe film before and after hydrogen ion irradiation was studied by means of X-ray diffraction (XRD). The XRD patterns for both doped and undoped samples, which are shown in the inset of Figure 1(a), did not show any peaks reflecting the amorphous nature of the deposited and irradiated films. The composition of the undoped films was checked by means of energy dispersive X-ray microanalysis (EDXA). The resulting dispersive curve is shown in the inset of Figure 1(b). The average atomic percentages of the amorphous InSe films were found to be $\sim$51% In and 49% Se. These ratios indicate that the grown films are composed of InSe only. The EDXA analysis of the doped films was not possible due to our lab instrumental limitations.

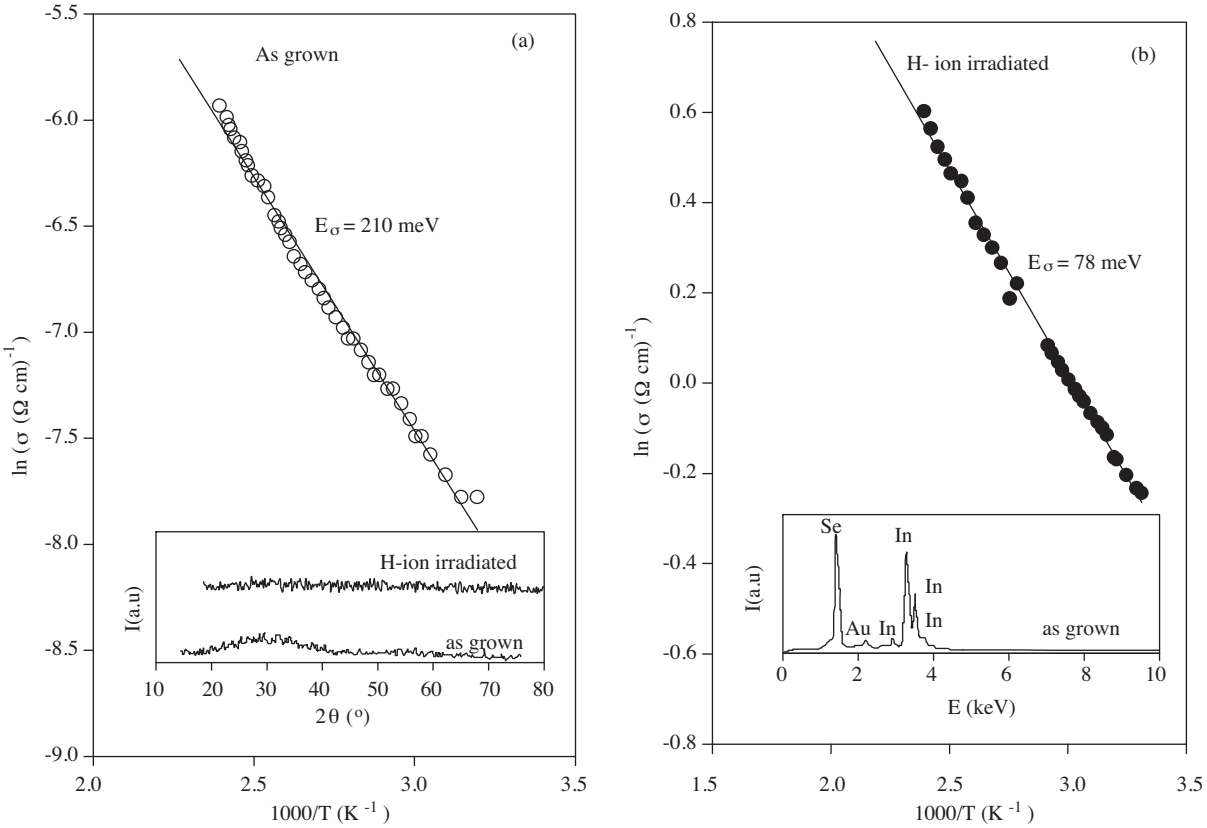

Figure 1. $\ln(\sigma)$ plotted as a function of T^{-1} for (a) as-grown and (b) hydrogen-implanted InSe films. The inset of (a) show the XRD results, and the inset of (b) shows the EDXA for the sample before implantation.

It is worth noting that the sample durability drastically decreased after H-ion implantation. Although we have no instrument that measures the samples durability before and after irradiation, one can observe the difference by eye. In contrast to it is natural case, the film can be cleaved easily from the substrate after irradiation.

The room temperature electrical conductivity σ values for the as-grown and irradiated samples were found to be 4.19×10^{-4} and 7.92×10^{-1} $(\Omega \cdot \text{ cm})^{-1}$, respectively. The decrease in the room temperature conductivity values by three orders of magnitude was also observed for Ge implanted GaSe crystals [12] and by two orders of magnitude for Si doped GaSe crystals [13]. Figures 1(a) and 1(b) show the variation of dark electrical conductivity as a function of reciprocal temperature in the temperature region of 300–420 K for the as grown and hydrogen ion implanted samples, respectively. As it can be seen in the plots, the conductivity values increase with increasing temperature. Change in the $\sigma - T^{-1}$ dependence is best expressed by the relation

$$\sigma = \sigma_0 \exp(-E_\sigma / kT). \tag{1}$$

Here, σ_0 and E_σ are the pre-exponential factor and the conductivity activation energy, respectively.

Typical best-fits for the experimental data are illustrated by the solid lines in Figures 1(a) and 1(b). The value of E_σ calculated from the slope of these lines were found to be 210 and 78 meV for the as-grown and hydrogen-implanted samples, respectively. Both energy values are less than half of the energy band gap indicating the extrinsic nature of conduction. The appearance of the 78 meV energy level in the band gap of

InSe films is due mainly to the hydrogen ion implantation which creates extra energy levels that contribute to the conductivity in this temperature region. Similar significant changes in the values of conductivity activation energies were also observed for Si implanted GaSe crystals. The activation energy for this crystal is observed to decrease from 243 to 158 meV by Si implantation [13].

Figure 2 shows variation of the absorption coefficient α as a function of incident photon energy E for as-grown and ion-implanted samples. The inset in the figure shows an enlarged portion of the absorption spectrum of the hydrogenated sample. The absorption coefficient was calculated from the relation

$$T = (1 - R)^2 \exp(-\alpha d). \tag{2}$$

In the above equation, d is the sample thickness, T is the measured transmittance and R is the computed reflectance. As it is clear from the Figure 2, the absorption coefficient of the as-grown samples exhibit a sharp decrease in the incident photon energy region of 1.81–1.51 eV. Namely, it decreases from 2.38×10^4 cm^{-1} at 1.81 eV to 1.46×10^4 cm^{-1} at 1.51 eV. The absorption coefficient of the hydrogen ion implanted sample decreases from 1.64×10^4 cm^{-1} at 1.66 eV to 1.45×10^4 cm^{-1} at 1.27 eV. This finding indicates clearly a sharp decrease in the value of the absorption coefficient associated with absorption edge shift by implantation. This shift, which was also observed for N-implanted GaSe [14] and for neutron transmutation doping of GaS and InSe semiconductors, was attributed to the extra levels introduced during the implantation and/or annealing above the valence band.

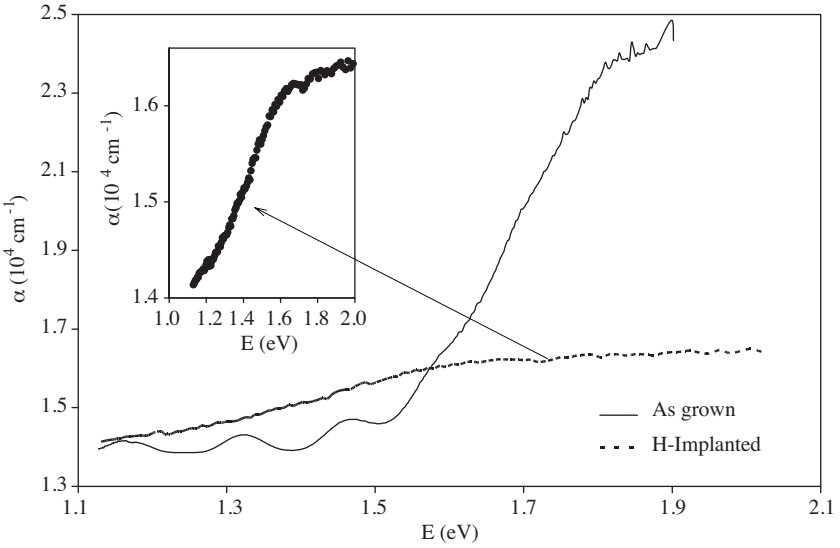

Figure 2. The room temperature absorption coefficient for the as-grown and implanted samples.

Following our previous work on the as-grown samples [11], the absorption coefficient can be analyzed by taking into account interband absorption theory, in which

$$(\alpha E) = B(E - E_g)^{1/2}. \tag{3}$$

Here, B is a constant and E_g is the direct allowed transition band gap energy [11]. Equation (3) is plotted in Figures 3(a) and 3(b) for the as-grown and H-implanted samples, respectively. The intercepts of the plots of $(\alpha E)^2$ versus E are found to be at 1.50 and at 0.97 eV for the as grown and H-implanted samples, respectively.

This sharp decrease in the value of the energy band gap was also observed for Cd doped amorphous GaSe films [15]. This decrease in band gap energy may be attributed to the valence band shift. Implantation of H atoms into InSe leads, possibly, to a distortion of the material valence band, resulting in a decrease of band gap energy. In addition to the H atoms insertion which increases the free carrier density in the samples, the difference in the values of the band gap reported here may also be attributed to many other reasons like the In/Se composition ratio and annealing temperatures (samples were kept at 200 °C during the implantation process).

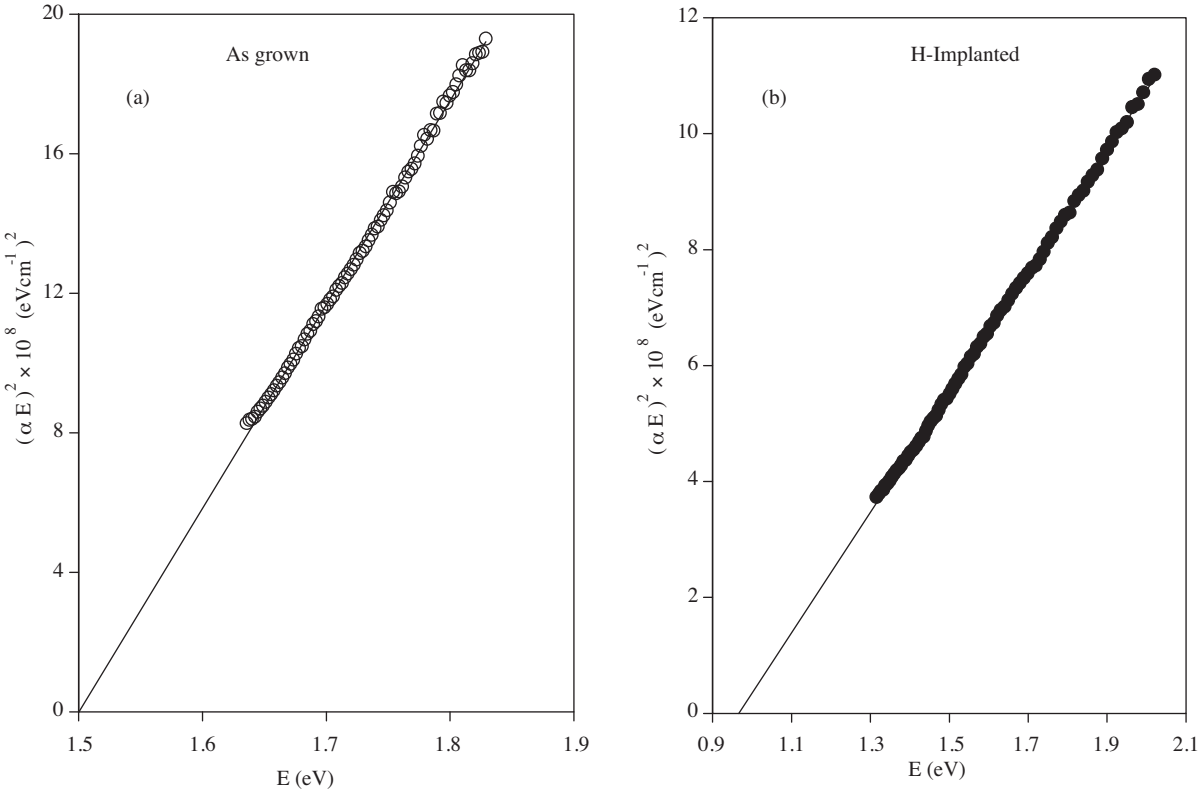

Figure 3. $(\alpha E)^2$ plotted as a function of E for the (a) as-grown and (b) H-implanted samples.

The energy gap of the as-grown sample is comparable with that reported in the literature. Particularly, Chaudhari et al. [16] reported a thickness dependent energy gap of 0.81–2.18 eV. Ateş et al. [17–19] reported an annealing dependence of energy gap being in the range of 1.33–2.08 eV. Consistently attenuation of the conductivity activation energy via annealing and substrate temperature was also observed [19–20]. Namely, the electrical conductivities of In_2Se_3 and InSe films are reported to be about $10^{-10}-10^{-7}$ and 10^{-6} $(\Omega\cdot\ \mathrm{cm})^{-1}$, respectively [19].

In the weak absorption region, the dispersive optical constants for the as-grown sample were previously calculated by using the Swanepoel method [21]. The data were published in [11]. To observe changes in the refractive index, oscillator and dispersion energy as well as that on the static dielectric constant of the as-grown sample by H-implantation, the reflectance R of the implanted sample was computed using equation (2) and assuming the validity of the relation $A + R + T = 1$ [21]. The refractive index of the H-implanted samples which is displayed in Figure 4(a) was calculated from the reflectance data in the incident wavelength region of 900–1100 nm. Using the same equations given in [3] and from the linear part of Figure 4(b), the refractive

index–wavelength variation leads to the determination of dispersion and oscillator energies as 4.23 and 1.60 eV, respectively. The static refractive index and static dielectric constant were also calculated as a result of the latter data and were found to be 1.91 and 3.64, respectively. Comparing the current calculated data with the previously published for the as grown sample [11, 22] as 25.05 and 2.97 eV, 3.07 and 9.43, and with that reported for Cd doped samples as 20.06 and 3.07 eV, 7.43 and 2.74, [10] a pronounced decrease in all the dispersive optical parameters is observable. These changes are attributed to the H-implantation which increases the number of free carriers in the samples.

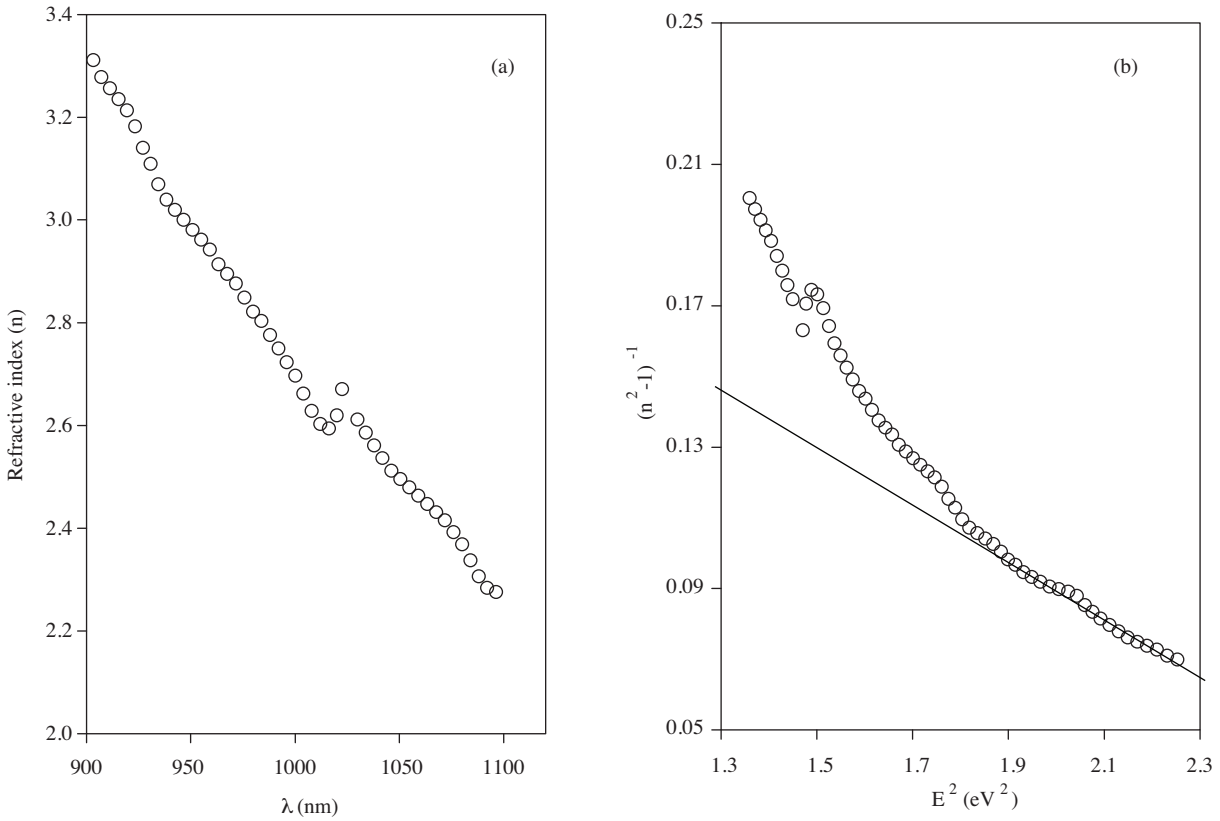

Figure 4. (a) Index of refraction n plotted as a function of wavelength λ for H-implanted InSe and (b) variation of $(n^2-1)^{-1}$ as a function of E^2.

4. Conclusions

In this study, amorphous indium selenide thin films have been deposited by thermal evaporation technique. After deposition the films were irradiated by hydrogen ion using an ion gun. The structural, electrical and optical properties of the implanted films are found to be strongly modified by H-implantation. Namely, the room temperature electrical conductivity decreased. This decrement is associated with a significant change in the value of the conductivity activation energy in which it is reduced from 210 meV to 78 meV by H-ion implantation. Consistently, the energy band gap of the films is reduced from 1.51 to 0.97 eV. Furthermore, the refractive index, dispersion and oscillator energy and static refractive index values are also observed to decrease by ion implantation. The above varieties are attributed to the increase in the carrier concentration in the samples which interns shifts the valence band up.

Acknowledgements

The authors would like to thank the B. Sc. student Ms. Estiklal Foqha for her help in the electrical data collection throughout her graduation project.

References

[1] G. Gordillo and C. Calderon, *Solar Energy Materials: Solar Cells*, **77**, (2003), 163.

[2] S. Marsillac and J. C. Bernede, *Thin Solid Films*, **315**, (1998), 5.

[3] J. C. Bernede and S. Marsillac, *Materials Research Bulletin*, **32**, (1997), 1193.

[4] V. N. Katerinchuk and M. Z. Kovalyuk, *Soviet Physics Semiconductors*, **25**, (1991), 577.

[5] D. Manno, M. D. Digiulio, T. Siciliano, E. Filippo and A. Serra, *Journal of Physics D: Applied Physics*, **34**, (2001), 2097.

[6] M. A. Kenway, A. F. El-Shazly, M. A. Afifi, H. A. Zayed and H. A. El-Zahid, *Thin Solid Films*, **200**, (1991), 205.

[7] V. M. Koshkin, L. P. Galchinetskii, V. M. Kulik and B. L. Minkove, *Solid State Communications*, **13**, (1973), 1.

[8] M. Balkanski, P. Gomes and R. F. Wallis, *Physica Status Solidi* (B), **175**, (1996), 194.

[9] A. F. Qasrawi, I. Gunal and C. Ercelebi, *Crystal Research and Technology*, **35**, (2000), 1077.

[10] A. F. Qasrawi, *Semiconductor Science and Technology*, **20**, (2005), 765.

[11] A. F. Qasrawi, *Optical Materials*, **29**, (2007), 1751.

[12] H. Karaağaç, M. Parlak, O. Karabulut, U. Serincan, R. Turan and B. G. Akınoğlu, *Crystal Research and Technology*, **41**, (2006), 1159.

[13] O. Karabulut, M. Parlak, K. Yilmaz, R. Turan and B. G. Akinoglu, *Crystal Research and Technology*, **38**, (2003), 1071.

[14] O. Karabulut, M. Parlak, R. Turan, U. Serincan and B. G. Akınoğlu, *Crystal Research and Technology*, **41**, (2006), 243.

[15] A. F. Qasrawi and A. A. Saleh, *Crystal Research and Technology*, **43**, (2008), 769.

[16] K. S. Chaudhari, Y. R. Toda, A. B. Jain and D. N. Gujarathi, *Advances in Applied Science Research*, **2**, (2011), 84.

[17] Aytunç Ateş , Mutlu Kundakçı, Aykut Astam and Muhammet Yıldırım, *Physica E*, **40**, (2008), 2709.

[18] S. N. Sahu, *Thin Solid Films*, **261**, (1995), 98.

[19] M. Yudasaka, T. Matsnoka and N. Nakanishi, *Thin Solid Films*, **146**, (1987), 65.

[20] B. Kobbi, D. Ouadjaout and N. Kesri, *Vacuum*, **62**, (2001), 321.

[21] R. K. Willardson and A. C. Beer, Semiconductors and semimetals, vol. 3, (Academic press, New York. 1967) p. 72.

[22] H. Bouzouita, N. Bouguila, S. Duchemin, S. Fiechter and A. Dhouib, *Renewable Energy*, **25**, (2002), 131.